https://doi.org/10.5194/egusphere-2026-2620
Preprint. Discussion started: 20 May 2026

Global and Regional Hydroclimatic Responses to Alternative Global Reforestation Pathways

Authors: Marzieh Mortezapour[1], Kirsten Zickfeld[1], Vivek K. Arora[2], Christine Leclerc[1]

[1]Department of Geography, Simon Fraser University, Burnaby, Canada
[2]Canadian Centre for Climate Modelling and Analysis, Environment and Climate Change Canada, Victoria, British Columbia, Canada
Correspondence to: Marzieh Mortezapour (marzieh_mortezapour@sfu.ca)

Abstract. Reforestation is a crucial component of climate change mitigation scenarios due to its potential to sequester CO2 from the atmosphere. In addition to its effect on atmospheric CO2, reforestation affects climate through changes in the surface energy and water balance. While the effects of large-scale reforestation on surface air temperature are well documented, its impact on the hydrological cycle remains underexplored. This study examines the global and regional hydrological consequences of two reforestation scenarios utilizing the CanESM5.1 Earth System Model: sustainable reforestation and a reversal of historical deforestation since 1850. Both scenarios are compared to a fixed land-cover baseline. We examine the components of the hydrologic cycle, cloud cover, and surface air temperature through simulations conducted from 2015 to 2200. Reforestation drives substantial regional variation in hydroclimatic responses. Higher latitudes experience warming in response to reforestation, whereas cooling dominates in low latitudes. Reforestation increases evapotranspiration in all regions, while precipitation and runoff responses vary by region. The results show that the hydrologic cycle continues to change in most regions long after tree cover has been restored, modulated by century-scale changes in large-scale atmosphere and ocean circulation. Our findings underscore the importance of reforestation strategies that jointly consider carbon sequestration and their effects on the water cycle.

1. Introduction

Reforestation and ecosystem restoration are increasingly promoted as nature-based solutions to help achieve net-zero emissions and the climate goal of the Paris Agreement (UNFCCC, 2015; IPCC, 2021). Reforestation offers co-benefits for biodiversity, land stewardship, and climate resilience in addition to its well-established role in carbon dioxide removal from the atmosphere (CDR) (Griscom et al., 2017). Beyond their carbon role, forest-cover changes also alter the water and energy cycles through variations in albedo, evapotranspiration (ET), surface roughness, and cloud formation (Mahmood et al., 2014; Devaraju et al., 2015; Duveiller et al., 2021).

Although the carbon benefits of reforestation are well documented (Robinson et al., 2025; Daley, 2024; Busch et al., 2024), its hydroclimatic consequences remain less certain and appear to be region and scale-dependent (Schwärzel et al., 2020; Buechel et al., 2024b). Global syntheses indicate that reforestation often exerts disproportionately bigger impacts on

https://doi.org/10.5194/egusphere-2026-2620
Preprint. Discussion started: 20 May 2026

streamflow compared to deforestation, highlighting the hydrological sensitivity to reforestation (Li et al., 2022). Recent modelling studies of the Earth system have begun to explore these hydroclimatic effects in greater depth.

Across multiple models, a consistent picture emerges of competing mechanisms. For example, simulations with CESM2 under SSP1-2.6 forcing show that afforestation/reforestation in the tropics yields cooling driven by heightened evapotranspiration. This increase in evapotranspiration can concurrently yield a decline in regional soil moisture and a decrease in water availability in certain forested regions (King et al., 2024). Similarly, European afforestation studies have demonstrated that forest expansion can moderate summer heat extremes while simultaneously reducing runoff or exacerbating water scarcity in certain dry regions (Asselin et al., 2024). Multi-model intercomparisons confirm that the sign and magnitude of these responses vary with local climate and geography, and tree-cover increases can either amplify or mitigate climate-driven runoff anomalies (Engel et al., 2025). These findings demonstrate the conflicting effects of increasing canopy water demand, referring to the enhanced transpiration and evaporative fluxes driven by vegetation under warmer or drier conditions, or decreased albedo, which can exacerbate drying, and increased ET and cloud feedback, which encourage cooling.

Model and satellite evidence further reveal the complexity of cloud responses. In some European regions, afforestation enhances low-cloud cover and surface reflectivity, producing a net cooling feedback (Caporaso et al., 2024), whereas other regional climate-model experiments show decreased cloud cover and a strengthening of albedo-driven warming, emphasizing model and region dependence (Breil et al., 2020).

At the global scale, reforestation influences atmospheric circulation beyond the reforested areas. Multi-model ensemble experiments indicate that tropical reforestation increases ET and local rainfall but frequently decreases net precipitation (P-E), particularly in western and southern Africa, where enhanced surface roughness from reforestation increases aerodynamic drag, weakening low-level convergence and thus offsetting the convective rainfall feedback from higher evapotranspiration (Fahrenbach et al., 2025). Similarly, Portmann et al. (2022) demonstrated that afforestation outside of the tropics can shift the Intertropical Convergence Zone (ITCZ), which in turn can change the distribution of rainfall patterns worldwide. Yet, multi-model intercomparison projects continue to reveal substantial structural uncertainty, differences arising from model formulations and parameterizations, in how land-use forcing translates into atmospheric and hydrological responses (De Hertog et al., 2022; Amali et al., 2025), while some studies report limited large-scale circulation responses (King et al., 2024). These disparities highlight the need for a deeper comprehension of regional effects as well as model sensitivity.

Regional and high-resolution analyses further emphasize spatial contrasts. Regional studies in humid regions such as the UK show that ET increases associated with reforestation/afforestation frequently outstrip precipitation gains, lowering streamflow (Buechel et al., 2022; 2024b). Conversely, a greater summer precipitation in reforested portions of continental Europe, ascribed to enhanced evapotranspiration and moisture recycling (Meier et al., 2021), implies that local hydrological feedbacks can partially offset water losses in some regions. Although the long-standing discussion over whether forests increase or decrease water yield remains unresolved, it is well understood that forests contribute to hydrological regulation by improving infiltration, stabilizing soils, and reducing rapid overland runoff (van Meerveld, 2025; Bruijnzeel, 2025). In their absence, more rainfall is lost as quick surface flow, which can heighten flood risks and limit groundwater replenishment. Forested landscapes, in contrast, facilitate slower infiltration and more sustained streamflow. However, recent global assessments show that reforestation can, in certain settings, lead to reduced groundwater recharge and lower

https://doi.org/10.5194/egusphere-2026-2620
Preprint. Discussion started: 20 May 2026

dry-season flows. Thus, while forests generally offer important hydrological benefits, reforestation efforts may also carry distinct hydrological implications in specific regions that merit careful consideration (van Meerveld, 2025; Bruijnzeel, 2025). Overall, these findings support the idea that forest-water interactions vary across spatial and temporal scales (Creed et al., 2019).

Finally, while afforestation-based CO_2 removal scales linearly with carbon uptake, its influences on the water and energy cycles are nonlinear and model-dependent (Moustakis et al., 2025). This emphasizes the importance of considering reforestation as a driver of hydrological and physical climate changes in addition to its potential as a climate change mitigation strategy. Collectively, the literature reveals persistent uncertainties in the magnitude and direction of hydroclimatic feedbacks to reforestation, especially beyond the 21st century and across contrasting land-cover strategies. To address these gaps, the present study employs the Canadian Earth System Model version 5.1 (CanESM5.1) to examine two different reforestation scenarios under SSP1-2.6 forcing: a "reversed" scenario that restores all of the forest that has been lost since 1850, and a "sustainable" scenario that emphasizes ecologically guided restoration in line with Natural Climate Solutions principles (Griscom et al., 2017; Cook-Patton et al., 2021). We assess long-term impacts of reforestation on temperature and water availability (defined here as the net balance between precipitation and evapotranspiration (P-ET)) through simulations extended to 2200, analyzing annual and seasonal timescales as well as zonal and regional spatial patterns to determine how the location of reforestation influences hydroclimatic outcomes.

2. Methods

2.1 Model Description

We use the Canadian Earth System Model version 5.1 (CanESM5.1; Arora et al., 2020; Swart et al., 2019) to assess the long-term climate and hydrologic impacts of large-scale reforestation. CanESM5.1 couples a ~2.8° atmosphere, a ~1° NEMO ocean, and interactive sea-ice, carbon cycle, and land surface components. The land surface is represented by the Canadian Land Surface Scheme (CLASS; Verseghy, 1991 and 2000; Verseghy et al., 1993), which simulates soil heat and moisture, snow accumulation and melt, and canopy-atmosphere fluxes. CLASS is coupled to the Canadian Terrestrial Ecosystem Model (CTEM; Arora, 2003; Arora and Boer, 2003 and 2005), which represents terrestrial carbon cycling and vegetation dynamics, including photosynthesis, respiration, phenology, and allocation across nine plant functional types. Vegetation physiology responds dynamically to changes in climate conditions (e.g., leaf area index, evapotranspiration, carbon fluxes), but the geographic distribution of the model's plant functional types (PFTs) is prescribed.

2.2 Experimental design

a) Reforestation scenarios

Three different land-use scenarios are used to investigate the effects of reforestation: (a) a reference scenario ("Baseline"), where land cover is specified at its year 2015 configuration and held fixed for the duration of the simulation; (b) a sustainable reforestation scenario ("sustainable"), which follows the global reforestation opportunity map developed by Griscom et al. (2017), which identifies areas suitable for restoration under natural climate solutions while accounting for biodiversity conservation and food-production safeguards; and (c) a reversed historical deforestation scenario ("reversed"), which restores forest cover to its year 1850 extent, replanting trees in areas where historical deforestation occurred. Changes

https://doi.org/10.5194/egusphere-2026-2620
Preprint. Discussion started: 20 May 2026

in historical land cover are guided by the changes in crop area from the Land Use Harmonization version 2 (LUH) dataset (Hurtt et al., 2020). LUH provides globally gridded, annually resolved land-use states and transitions from 1850 to 2015. It harmonizes historical reconstructions of cropland, pasture, forest, and urban land with future scenarios, ensuring continuity across the historical-future boundary. In our experiments, we used LUH data to represent the historical evolution of cropland expansion and associated forest loss. These cropland-driven changes served as the basis for defining the 'reversed' reforestation scenario, in which forest cover is restored on lands that were converted to cropland after 1850. In both cases, tree cover is prescribed to increase linearly between 2015 and 2070 (Fig. S1). Both reforestation scenarios expand global tree cover by roughly 7 Mkm² (Reversed: 6.6 Mkm²; Sustainable: 6.3 Mkm²), consistent with the observed decline in forest area from 75 Mkm² in 1850 to 68 Mkm² in 2015. While the extent of tree cover changes in the two reforestation scenarios is similar, the specific locations of reforestation differ (Fig.1), which allows us to investigate the sensitivity of the hydroclimate response to changes in the spatial pattern of reforestation.

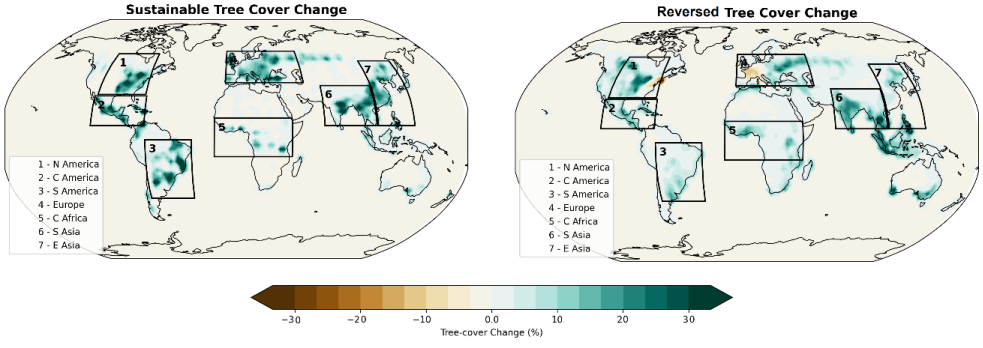

Figure 1. Percentage increase in forest cover from 2015 to 2070, with boxes indicating the different regional domains, for two land-cover scenarios: sustainable and reversed historical reforestation.

b) Model experiments

The historical simulation was initialized from a pre-industrial control run, ensuring equilibrium conditions prior to the onset of anthropogenic forcing. The historical period covers 1850-2014, following CMIP6 protocols, and is seamlessly extended by scenario simulations from 2015 to 2200. All scenario simulations follow the SSP1-2.6 pathway and its extension for CO_2 concentrations (Meinshausen et al., 2020), non-CO_2 greenhouse gas and aerosol forcings. Because atmospheric CO_2 concentrations are prescribed rather than responding to the respective land-cover scenario, any changes in hydroclimate in the reforestation relative to the baseline simulations arise solely from biogeophysical effects of land-cover changes. For each land-use scenario (baseline, sustainable, and reversed), we performed simulations for five ensemble members (n = 5). Ensemble members were generated by applying small perturbations to ocean initial states at the end of the historical simulation, which preserves consistency in external forcing while sampling internal variability. This ensemble design allows us to isolate the forced hydroclimatic response of land-use change from background variability.

2.3 Model data analysis

https://doi.org/10.5194/egusphere-2026-2620
Preprint. Discussion started: 20 May 2026

To quantify the effects of land-cover change on the hydroclimate, we analyze differences in key hydroclimatic variables between the reforestation and baseline simulations. The variables are grouped into (i) surface energy balance components (surface temperature, albedo, radiation fluxes, cloud fraction), (ii) hydrological components (precipitation, evapotranspiration, runoff, soil moisture, and P-E), and (iii) large-scale circulation diagnostics (Hadley circulation, the Atlantic Meridional Overturning Circulation: AMOC). Regional means are calculated for seven domains: North America, Central America, South America, Europe, Central Africa, South Asia, and East Asia (Fig.1). Zonal and global diagnostics are also investigated. Variables are analyzed on annual and seasonal timescales. Statistical significance of anomalies relative to the baseline is assessed using a Wilcoxon signed-rank test at α=0.05. All results are presented as ensemble means, with variability across members providing a measure of robustness in the simulated signals.

Analysis is focused on three periods: near term (2025; 2015-2035), end of century (2100; 2090-2110), and long term (2190; 2180-2200). Most differences are evaluated relative to the baseline simulation. Temporal changes are expressed relative to the 2025 climatology and normalized by reforested area (Mkm²) where relevant.

3. Results

3.1. Temperature Response

To evaluate the climatic effects of reforestation, we analyzed variations in surface air temperature between the sustainable and reversed reforestation scenarios relative to the baseline with constant year-2015 land cover using ensemble averaged results. Both reforestation scenarios produce broadly consistent spatial patterns in near surface (2m) air temperature relative to the fixed land cover baseline. In the tropics, increased tree cover yields widespread cooling and higher cloudiness across South America, Central Africa, and Southeast Asia. At mid- and high latitudes, particularly in the Northern Hemisphere, new forest cover in snow affected regions reduces albedo, resulting in surface warming that is often accompanied by slight reductions in total cloud fraction. These similarities highlight the dominant biophysical mechanisms of reforestation: evaporative and cloud mediated cooling in low latitudes and albedo driven warming in high latitude regions.

While the broad patterns of cooling in low latitudes and warming in high latitudes are consistent across both scenarios, the magnitude and spatial extent of these anomalies differ between sustainable and reversed reforestation scenarios, with the reversed scenario exhibiting both amplified warming in high latitude zones and cooling or wetting signals in the tropics compared to the sustainable scenario (Fig.2). In the sustainable reforestation scenario, local responses are strongest within reforested tropical and subtropical regions. South America, Central Africa, and both Southeast Asia exhibit cooling of -0.5 to -1.0 °C, coinciding with statistically significant increases in total cloud fraction over the same regions. This suggests that enhanced evapotranspiration promotes both evaporative cooling and greater cloudiness, which in turn reduces incoming shortwave radiation and reinforces the surface cooling (Fig. S3). Remote effects are weaker but detectable relative to the baseline scenario: high latitudes show small positive anomalies (<+0.3 °C), largely confined to North America and Eurasia. The cloud anomalies in remote areas are minimal or insignificant. Although equatorial regions cool locally, the zonal mean reveals that warming at higher latitudes outweighs tropical cooling, giving a net poleward amplified warming pattern.

https://doi.org/10.5194/egusphere-2026-2620
Preprint. Discussion started: 20 May 2026

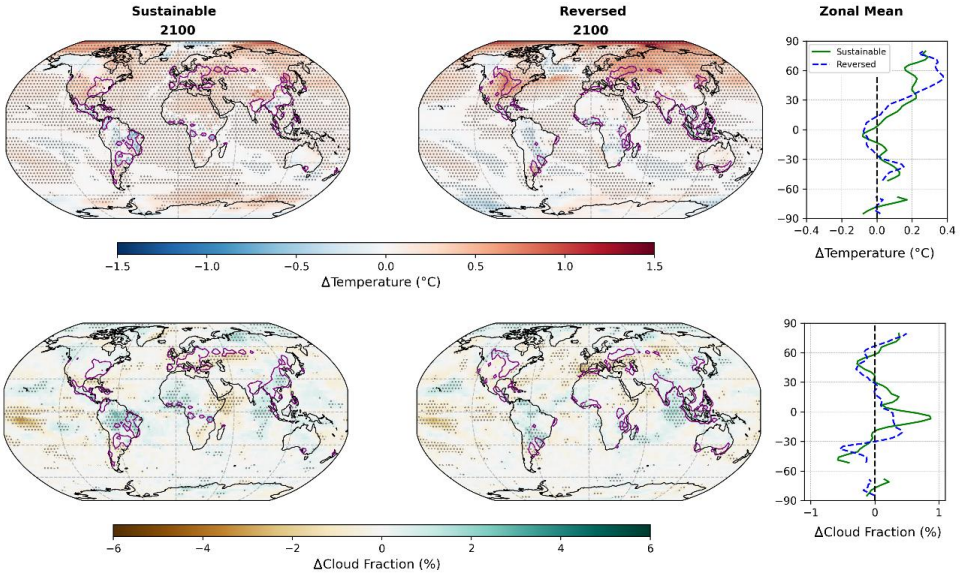

Figure 2. Top) 2m Air temperature (°C) and bottom) cloud fraction (%) differences at year 2100 (2090-2110) for two land cover scenarios (sustainable and reversed historical reforestation) compared to the baseline with fixed year 2015 land cover. Gray dots indicate statistically significant differences at p < 0.05 based on a Wilcoxon signed rank test. Zonal means are calculated over land only grid cells using 10° latitude bands. The purple contour lines delineate regions where the change in tree cover exceeds 10%.

The reversed reforestation scenario shows stronger and more spatially extensive anomalies. In tropical reforested zones, cooling persists in equatorial regions (-0.5 to -1.0 °C), while increases in cloud fraction are more spatially variable and often not statistically significant, reducing the robustness of the signal compared to the sustainable case. In contrast, mid and high latitude reforestation produces robust warming: North America, Europe, and Eurasia warm by +0.5 to +1.0 °C, with winter and spring peaks exceeding +1.2 to +1.5 °C (Fig. S2). These signals are statistically significant across large areas, reflecting strong albedo feedbacks from new forests established on snow covered ground. The pronounced warming observed at mid and high latitudes, particularly in regions of newly established forest, aligns with established biophysical feedback mechanisms: when forests decrease the albedo of snow reflective surfaces, leading to more solar energy being absorbed, triggering a positive albedo-snow feedback that amplifies warming in high latitude zones (Abe et al., 2017; Bright et al., 2017). Remote effects include modest but widespread reductions in total cloud fraction across the Northern Hemisphere extratropics through adjustments in circulation and energy transport (Portmann et al., 2022), which allow more incoming solar radiation to reach the surface and reinforce the warming (Cho et al., 2018; Luo et al., 2024). In the tropics, by contrast, enhanced latent heat flux and cloud shading counter albedo induced surface warming, driving the observed cooling signal in reforested areas.

3.2. Hydrological Cycle Response

https://doi.org/10.5194/egusphere-2026-2620
Preprint. Discussion started: 20 May 2026

The hydrological cycle shows broadly consistent features across both sustainable and reversed reforestation scenarios, with reforested tropical regions generally experiencing increases in precipitation and evapotranspiration (Fig.3).

a) Local responses in reforested regions

In both scenarios, enhanced vegetation with greater canopy interception and transpiration promotes higher evapotranspiration fluxes over reforested areas. These responses align with observed and modelled effects of forest recovery, where canopy interception, leaf area expansion, and root mediated access to soil moisture jointly contribute to elevated evapotranspiration (e.g., Bonan, 2008; Ellison et al., 2012; Zhang et al., 2017). These changes are consistent with statistically significant anomalies in evapotranspiration in many tropical land areas. Outside the tropics, anomalies remain generally weak, including over reforested areas, highlighting the considerable geographic dependency of hydrological changes. In both land cover scenarios, evapotranspiration increases over areas of forest expansion, but the distribution differs. The sustainable scenario shows broadly distributed yet moderate ET gains of about +0.1-0.3 mm day^{-1} across tropical regions, whereas the reversed scenario produces stronger and more localized ET increases (up to +0.4-0.6 mm day^{-1}), especially over the Southern America and Congo basins. This intense regional feedback suggests that most of the added rainfall is recycled through evapotranspiration.

Despite consistent spatial patterns, the magnitude, spatial extent, and regional balance of responses in precipitation differ between scenarios. Sustainable reforestation causes moderate increases in precipitation in tropical regions with slight to moderate increases of up to +0.3-0.5 mm day^{-1} across reforested tropical regions such as South America and central Africa. Outside the tropics, changes remain minimal ($\leq \pm 0.1$ mm day^{-1}). This enhancement coincides spatially with areas of elevated evapotranspiration and is accompanied by increases in near surface specific humidity (not shown), suggesting that local moisture recycling contributes to the precipitation response. While this spatial coherence supports a recycling driven mechanism, we cannot fully exclude a role for large scale circulation changes. The reversed reforestation scenario, on the other hand, results in more diverse precipitation responses: localized increases exceed +0.5 mm day^{-1} in South and East Asia, especially during JJA, while reductions of -0.2 to -0.3 mm day^{-1} occur in southern America and West Africa up to -0.6 to -0.8 mm day^{-1} in DJF and MAM (Fig. S4).

Runoff responses diverge strongly between regions: decreases of -0.2 to -0.3 mm day^{-1} in subtropical South America and West Africa reflect greater canopy water demand, while increases of +0.3-0.5 mm day^{-1} occur in Southern America and parts of Asia. These anomalies are statistically significant in several regions, particularly the drying in West Africa and the wetting in East Asia, indicating robust regional hydroclimatic contrasts.

https://doi.org/10.5194/egusphere-2026-2620
Preprint. Discussion started: 20 May 2026

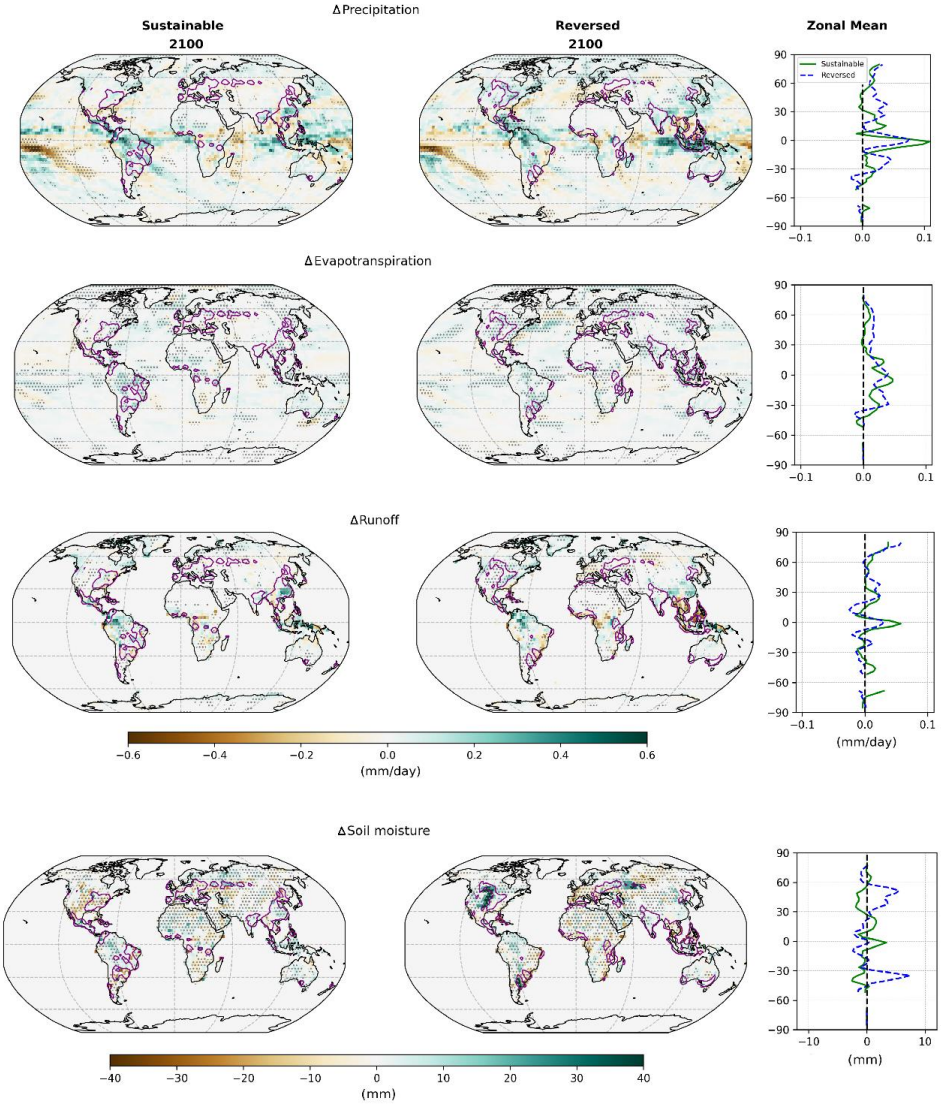

Figure 3. From top to bottom: precipitation, evapotranspiration, runoff changes in (mm day^{-1}), and soil moisture difference in (mm) at 2100 (2090-2110) for two land cover scenarios (sustainable and reversed historical reforestation) compared to the baseline with fixed year 2015 land cover. Gray dots indicate statistical significance of differences assessed using a Wilcoxon test at $p < 0.05$; Land only zonal 10 degree means of the differences are shown on the right. The purple contour lines delineate regions where the change in tree cover exceeds 10%.

Both scenarios show a common pattern of modest reduction in soil moisture in subtropical regions reflecting increased evaporative demand under warmer conditions (Fig.2). While both scenarios show moisture deficit during JJA and SON, the

https://doi.org/10.5194/egusphere-2026-2620
Preprint. Discussion started: 20 May 2026

magnitude and spatial extent differ strongly. Under the sustainable scenario, soil moisture anomalies remain relatively small across most regions (generally within ±10 mm), with localized increases in tropical South America and Central Africa during DJF and MAM, consistent with enhanced precipitation. In contrast, the reversed scenario produces much stronger and more widespread drying signals, particularly in South America, West Africa, and South Asia, where deficits reach -20 to -40 mm, especially in DJF and MAM. High latitude North America and Eurasia show opposite behaviour, with seasonal soil water gains of +20 to +30 mm linked to remote climate driven changes in snow accumulation and melt, which enhance infiltration and reduce runoff (Fig. S5).

b) Remote and non-local responses

Outside the tropics, precipitation changes remain generally weak, with high latitude responses showing only small and mostly insignificant anomalies (Fig.3). Remote effects are therefore limited in the sustainable scenario, although the zonal mean reveals a narrow tropical precipitation increase between ~10°S-10°N (Fig. S4).

There is little evidence of ITCZ displacement or hemispheric asymmetry in the precipitation field (Fig. S4). Remote effects are more evident in the reversed scenario, where the zonal mean indicates a dipole pattern, with enhanced precipitation in the Southern Hemisphere tropics and reduced rainfall across 0-10°N (Fig. S4), suggesting ITCZ-related adjustments. High latitude regions also exhibit small positive runoff anomalies (+0.1-0.2 mm day^{-1}), likely linked to snowmelt and earlier spring discharge (Fig. S5). Latitudinal differences have also been shown in the hydrologic response: recent global analyses indicate that decreases in runoff primarily occur in water limited or seasonally dry tropical regions, while increases in evapotranspiration are more pronounced in humid regions (De Hertog et al., 2022; Hou et al., 2023).

3.3. Regional Surface Water Budget Changes

Reforestation modifies regional water budgets through combined changes in precipitation (P), evapotranspiration (ET), runoff (R), and soil moisture (SM). These hydrological changes can be interpreted using the terrestrial water budget equation,

$$dS/dt = P - ET - R$$

In which S denotes the combined storage of soil moisture and snow. Because the extent of reforested land varies across regions and scenarios, hydrological anomalies are normalized by the reforested area (Mkm²; defined as grid cells with >10% tree cover increase). This normalization expresses changes per unit reforested land, allowing consistent comparison of hydrological responses across regions with different levels of reforestation. The fluxes are evaluated for 2100 (2090-2110) relative to the fixed land cover baseline (Figs.4, S5, S6). In nearly all regions, ET increases following forest expansion. Precipitation also rises modestly in most regions (≤+0.2 mm day^{-1} per Mkm² of reforested area), except Central Africa, where both scenarios show persistent declines of up to -0.1 mm day^{-1} per Mkm² of reforested area. Changes in precipitation in South Asia remain largely neutral. Despite similar broad patterns of increasing P-ET in all regions except in South America and Central Africa, the magnitude and distribution of P-ET changes diverge between scenarios. Central America shows particularly strong precipitation gains (+0.2 to +0.3 mm day^{-1} per Mkm² of reforested area), coupled with enhanced P-ET under the reversed scenario. South America emerges as the region of greatest contrast between scenarios: while

https://doi.org/10.5194/egusphere-2026-2620
Preprint. Discussion started: 20 May 2026

sustainable reforestation produces near neutral anomalies, the reversed case shows significant runoff and P-ET deficits of -0.2 to -0.3 mm day^{-1} per Mkm², indicating reduced P-ET, despite higher rainfall.

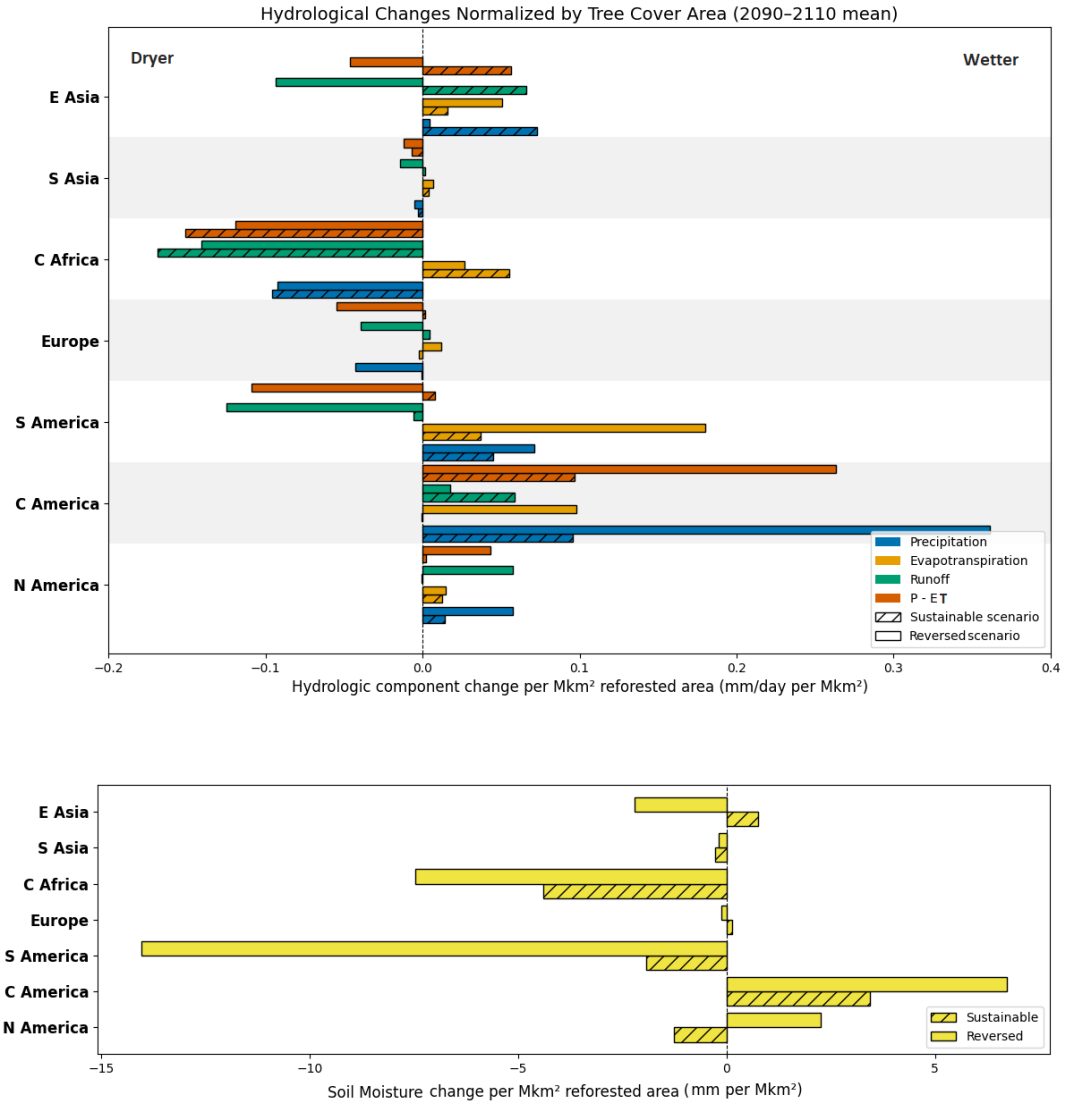

Figure 4. Top) Hydrological flux changes (mm day^{-1}) and bottom) Soil moisture changes (mm) for seven regions normalized by reforested area in km² in 2100 (2090-2110) compared to the baseline scenario with fixed land cover.

Consistent with runoff responses, soil moisture responses further emphasize this contrast. Both scenarios produce widespread drying in tropical and subtropical regions, with anomalies of -5 to -10 mm per Mkm² of reforested area, but the

https://doi.org/10.5194/egusphere-2026-2620
Preprint. Discussion started: 20 May 2026

largest deficits occur under reversed reforestation, reaching -15 mm per Mkm² in South America and Central Africa, particularly during DJF and MAM (Figs. S5, S6). In contrast, Central America exhibits small soil moisture gains, and North America shows slight increases under the reversed scenario (+2 to +3 mm per Mkm² of reforested area), likely linked to cooler, wetter conditions in high latitude regions. The reversed reforestation scenario produces more heterogeneous seasonal responses: South America shows wetter conditions in SON and drier conditions in DJF, while Central Africa and South Asia experience increased precipitation during winter and spring but reduced runoff overall (Figs. S5, S6). East Asia exhibits strong increases in both precipitation and ET during MAM, whereas Europe remains consistently near neutral in terms of precipitation and hydrological fluxes. These values represent changes integrated over the CLASS soil column, which spans approximately 4 m. Although the soil moisture anomalies represent a relatively small fraction of the total soil water column, they are large enough to influence surface fluxes and land-atmosphere coupling and are therefore climatologically meaningful.

3.4. Long term Effects

In both scenarios, hydroclimatic anomalies continue to evolve after 2100, with several common large scale features emerging (Figs. 5 and 6). Zonal means reveal reduced warming at high latitudes, with temperature increases tapering down to below +0.1 °C at 70-80°N by 2200. Precipitation consistently decreases north of the equator (0-10°N, -2 to -4%) while increasing across the Southern Hemisphere tropics and subtropics (0-30°S, +1 to +3%), indicating a southward displacement of the ITCZ (Fig. S7). These precipitation patterns are accompanied by modest but sustained anomalies in evapotranspiration (+1-2% in the tropics) and runoff (-0.5 to -1% north of the equator), while soil moisture shows opposing tendencies, with declines of -2 to -5 mm (0.8-1.5%) in the Northern Hemisphere tropics and gains of up to +2 mm (0.5-1%) in the Southern Hemisphere.

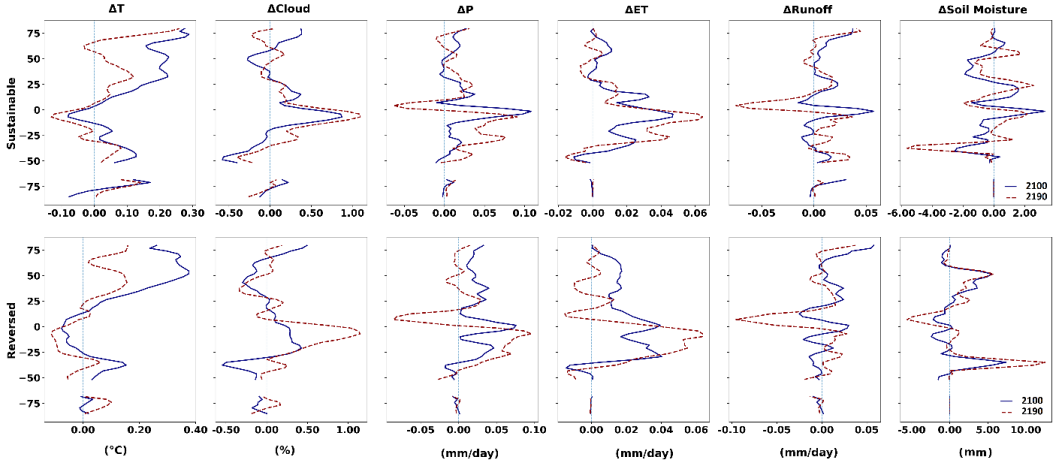

Figure 5. Zonal mean changes (10 degree mean) in hydroclimatic variables in the reforested area for the two reforestation scenarios. The changes are calculated as the difference between 2100 (2090-2110 mean; blue line) and 2190 (2180-2200 mean; dashed red line) for each scenario and the baseline simulation over land regions. Note that the scale differs between plots.

https://doi.org/10.5194/egusphere-2026-2620
Preprint. Discussion started: 20 May 2026

Although the area weighted mean values (Fig.6) show that both scenarios alter global hydroclimate in similar ways, the reversed reforestation pathway produces a substantially stronger and more spatially uneven response. By 2200, precipitation declines of more than -4% north of the equator coincide with intensified Southern Hemisphere wetting (+3-4%), reflecting a strengthened meridional moisture gradient. These shifts translate into larger land-surface impacts: soil moisture deficits in Southern America, West Africa, and South Asia reach -5 mm, more than double those under the Sustainable scenario. In contrast, the Sustainable pathway generates smaller anomalies and more even latitudinal distribution across hemispheres, with modest tropical increases in precipitation and evapotranspiration (+1-2%) largely balancing each other, resulting in little net change in P-ET at the global scale. This contrast indicates that the Reversed case amplifies hemispheric asymmetries in hydroclimatic responses to reforestation, whereas the Sustainable case maintains a near zero net water balance by 2200.

The persistence and amplification of these patterns beyond 2100 underscore the increasing role of large scale atmosphere-ocean circulation in shaping the long term hydroclimatic response. After 2100, the hydrological components continue to evolve, driven primarily by changes in the Hadley circulation and the Atlantic Meridional Overturning Circulation (AMOC). As shown in Figure S7, a weakened AMOC reduces northward ocean heat transport, leading to cooling of the Northern Hemisphere and a compensatory southward shift of the Intertropical Convergence Zone (ITCZ). This thermodynamic adjustment, consistent with energy balance considerations and supported by prior modelling studies (Frierson et al., 2013; Green & Marshall, 2017), is accompanied by a broadening and southward displacement of the Hadley cell by approximately 5-10° latitude. These circulation changes reinforce a meridional precipitation dipole, suppressing moisture convergence in the subtropical Northern Hemisphere and enhancing it in the Southern Hemisphere, which increasingly dominates the late century hydrological response and exceeds the direct biophysical impacts of land cover change alone.

https://doi.org/10.5194/egusphere-2026-2620
Preprint. Discussion started: 20 May 2026

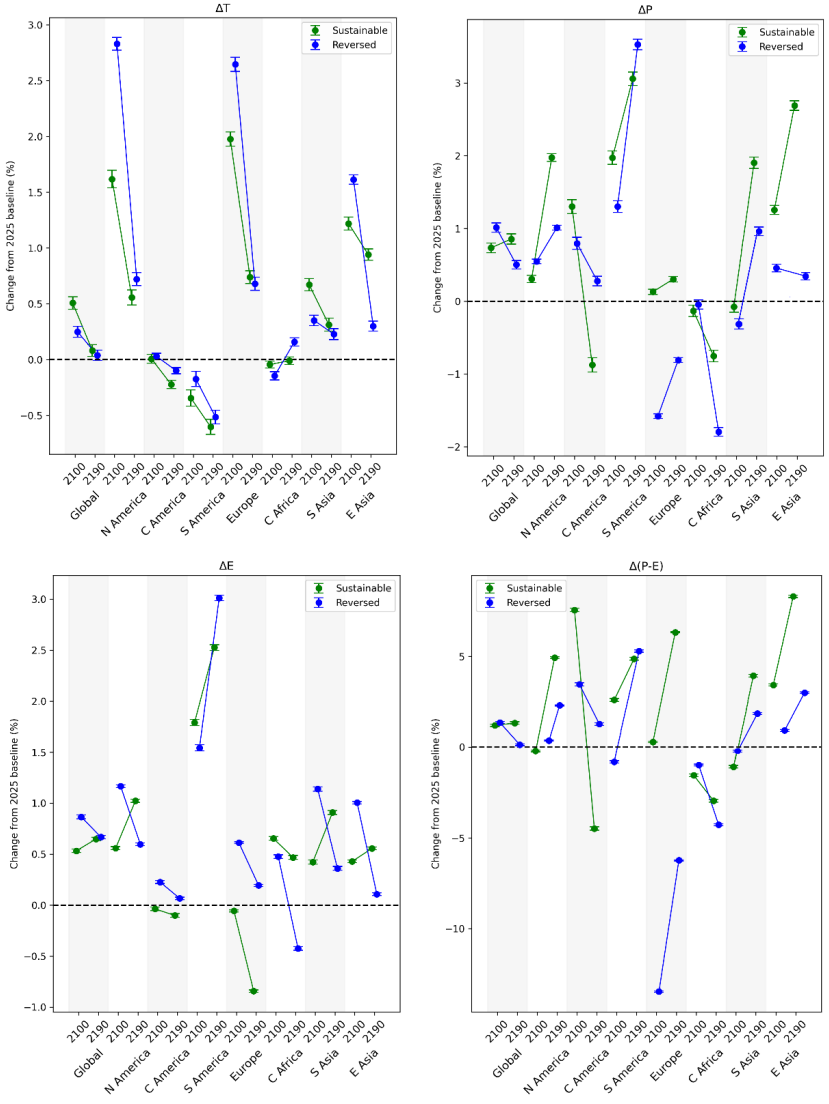

Figure 6. Area weighted mean values for 2m air temperature, precipitation, evapotranspiration, and P-ET, for grid cells where the increase in tree cover between 2015 and 2070 exceeds 10 %, expressed as percentage differences from 2025 mean for the baseline with fixed land cover globally and for 7 regions: North America, Central America, South America, Europe, Central Africa, South Asia, and East Asia. For each land cover scenario, the left point indicates the 2100 (2090-2110) mean and the right point the 2190 (2080-2200) mean. Note that each plot has a different scale.

4. Discussion

https://doi.org/10.5194/egusphere-2026-2620
Preprint. Discussion started: 20 May 2026

This study used simulations with CanESM5.1 to examine how two reforestation pathways, a sustainable reforestation pathway and a pathway that reverses historical deforestation, modify surface energy balance, clouds, and the water cycle from 2015 to 2200 relative to a fixed land cover baseline.

4.1. Energy balance and temperature responses

Across scenarios, expansion in tree cover increases evapotranspiration and latent cooling in the tropics, while albedo reductions in snow affected regions enhance net downward short wave radiation and, as a consequence, result in warming at high latitudes. The net outcome is a robust regional contrast: cooling in low latitude reforested areas and warming in mid to high latitude Northern Hemisphere regions. This pattern reflects the latitudinal placement of forest expansion rather than differences in total restored areas, which are similar between scenarios.

Beyond the direct local cooling over newly forested tropical land, both scenarios also generate remote temperature responses, most notably enhanced warming over the Arctic and northern mid latitudes, consistent with previous studies showing that land surface changes can modify large scale energy transport and circulation patterns (Brovkin et al., 2006; Swann et al., 2010; Winckler et al., 2019; Davin and de Noblet-Ducoudré, 2010). These remote responses reflect coupled atmosphere-ocean adjustments that extend beyond local land-surface biogeophysical effects. In particular, warming in Northern Hemisphere extratropical regions reflects the combined influence of land-atmosphere feedbacks and large scale energy redistribution, whereas temperature anomalies over the Southern Hemisphere extratropics remain comparatively weak, consistent with the smaller land fraction and more efficient ocean heat uptake.

4.2. Cloud responses

Cloud responses exhibit distinct regional patterns that mirror the temperature anomalies in both scenarios. In the tropics, reforested areas show small but consistent increases in cloud fraction, especially over Southern America, Congo Basin, and Southeast Asia, associated with enhanced evapotranspiration and boundary layer moisture. In contrast, at mid and high latitudes, cloud fraction anomalies remain weak and spatially heterogeneous with little sustained increase over mid and high latitude reforestation regions. Rather, cloud formation is suppressed by drying and subsidence in subtropical regions, especially in North Africa, where the greatest cloud reductions take place. In general, cloud feedbacks reinforce cooling in the tropics and have less effect in high latitudes, amplifying but not dominating the surface temperature response.

Previous modelling and observational studies showed that the biogeophysical response to reforestation is strongly latitude dependent: tropical forests generally enhance cloud formation through increased evapotranspiration and moisture convergence, whereas mid and high latitude forests exert a weaker or even opposite effect because surface albedo changes dominate the radiative balance. This pattern is consistent with our findings (Cerasoli et al., 2021; Xu et al., 2022; Portmann et al., 2022).

4.3. Hydrological responses and regional contrasts

Hydrological responses under both scenarios share some common features. In nearly all regions, evapotranspiration increases, reflecting enhanced canopy transpiration, while precipitation also tends to rise moderately, except in Central Africa. Despite these similarities, the balance between fluxes differs by location, producing regionally distinct outcomes.

https://doi.org/10.5194/egusphere-2026-2620
Preprint. Discussion started: 20 May 2026

Although modest in absolute magnitude relative to climatology, these anomalies are hydrologically significant because they persist over large areas and multiple decades. A range of recent studies (Hoek van Dijke et al., 2022; Zan et al., 2024; Dubois et al., 2023; Li et al., 2024) similarly show that the hydrological effects of reforestation depend strongly on where forests are restored.

Reforestation can lead to contrasting hydrological responses across regions. In some water limited or seasonally dry settings, enhanced evapotranspiration may reduce mean runoff, whereas in humid and cooler climates, forests often increase soil moisture and water availability. At the same time, forests can support local and regional precipitation through precipitation recycling, enhance subsurface water storage, and dampen streamflow seasonality by releasing water more gradually. As a result, the hydrological impacts of reforestation are spatially heterogeneous and may appear as regional "winners" and "losers," reflecting differences in climate regime, scale, and hydrological metrics rather than an overall negative effect of forest expansion.

4.4. Drivers of remote effects (ITCZ and circulation)

Our results confirm our hypothesis that variations in the geographic location of forest expansion are the main cause of the different hydrological responses under the sustainable and reversed reforestation approaches. A modest southward shift of the Intertropical Convergence Zone (ITCZ) emerges after 2100, indicating basin scale adjustments in the large scale circulation. Hadley cell differences show a broader ascent footprint into the Southern Hemisphere with slightly stronger subsidence north of the equator. In the reversed case, the spatial extent of the ascent anomaly grows, but the peak vertical velocity anomaly is not stronger than at 2100, suggesting a lateral shift or expansion rather than intensification. Concurrent AMOC diagnostics point to a small weakening in the reversed scenario by 2200, consistent with reduced northward ocean heat transport and compensating southward atmospheric energy transport, which would favour a southward shifted ITCZ. While these dynamical anomalies are modest in amplitude, their hydrological imprint is appreciable because even small ITCZ shifts reorganize basin scale rainfall.

These patterns are consistent with previous studies. Portmann et al. (2022) showed that large scale land cover change can shift the ITCZ through coupled atmosphere-ocean energy exchanges, and Fahrenbach et al. (2025) demonstrated that tropical afforestation can induce remote hydroclimatic responses through changes in cross equatorial energy transport. More broadly, these patterns are consistent with multi model studies (Hoek van Dijke et al., 2022; Dubois et al., 2023; Zan et al., 2024) and align with King et al. (2024), who highlighted persistent regional hydrological trade offs.

4.5. Limitations

Several limitations frame the interpretation of our results. Although we use five ensemble members, many regional changes remain statistically insignificant. The analysis relies on a single Earth System Model configuration and does not account for structural uncertainty (Amali et al., 2025; De Hertog et al., 2022). Vegetation physiology responds dynamically, but geographic distribution is prescribed, and disturbances are not included (Hou et al., 2023). Finally, we assess two end member pathways that differ in spatial distribution rather than total area, which may miss intermediate or regionally specific variants. These limitations suggest that our results should be interpreted as process level insights rather than precise regional projections.

https://doi.org/10.5194/egusphere-2026-2620
Preprint. Discussion started: 20 May 2026

4.6. Policy implications

The policy relevance of these findings lies in the sensitivity of biogeophysical outcomes to where forests are restored. Reforestation in snow covered northern regions contributes to high latitude warming through albedo effects, while reforestation in water limited or convection sensitive regions can reduce water availability. In contrast, reforestation in humid regions results in smaller hydrological and thermal anomalies. These results reflect long term mean states and do not account for processes such as reduced streamflow seasonality, flood attenuation, and enhanced soil stability. Reforestation also provides ecological co-benefits, including biodiversity enhancement, improved soil functioning, and ecosystem services (Poorter et al., 2016; IPBES, 2019; Lal, 2018; FAO, 2020; Bonan, 2008; Griscom et al., 2017).

These findings are consistent with global assessments showing that tree restoration can enhance water supply in some regions while reducing it in others (Hoek van Dijke et al., 2022; Zan et al., 2024). This has direct implications for climate policies: carbon gain alone is not sufficient to ensure co-benefits for water resources. Reforestation planning must account for spatial context, and future research should prioritize multi model comparisons and basin scale assessments to better quantify these impacts.

5. Conclusions

Using CanESM5.1, we evaluated the long term hydroclimatic consequences of two reforestation scenarios under SSP1-2.6 forcing: a sustainable pathway and a pathway with “reversed” reconstruction of historical deforestation. Across both scenarios, tree cover expansion enhances evaporative cooling in the Tropics and produces surface warming at high latitudes due to reduced albedo over snow affected regions. This latitudinal contrast, tropical cooling and high latitude warming, emerges consistently across both pathways and reflect the geographic sensitivity of biogeophysical feedbacks rather than differences in total restored forest area.

Hydrological responses to reforestation show consistent large scale patterns across both pathways. Tropical regions exhibit slight increases in precipitation and evapotranspiration, while high latitude regions tend to experience warming associated declines in soil moisture. Seasonal analyses indicate that the most pronounced hydrological shifts occur during high latitude winter and spring, when land-atmosphere coupling is strongest and background climate gradients are steepest. Although global mean anomalies in P-ET and runoff remain small, regional impacts on water availability can be significant, particularly in areas where reforestation intersects with existing hydroclimatic stress.

Beyond 2100, both scenarios continue to evolve, highlighting the need to examine timescales beyond the 21st century. Sustainable reforestation stabilizes, with anomalies remaining small and balanced, whereas reversed reforestation sharpens regional inequalities, notably long term reductions in Central African P-E. Zonal means reveal a dipole of drying across 0-10°N and wetting across 0-30°S by 2200, consistent with a modest southward ITCZ shift supported by Hadley cell and AMOC anomalies. While these circulation changes are limited in amplitude, they nevertheless reorganize rainfall over basin scales, underscoring the capacity of reforestation to influence large scale climate dynamics on centennial horizons.

Overall, our results show that the spatial distribution of reforestation plays a central role in shaping its hydroclimatic effects. Across both pathways, reforestation enhances evaporative cooling in the tropics and increases surface warming in snow affected northern regions, while global mean hydrological changes remain relatively small. However, regional outcomes

https://doi.org/10.5194/egusphere-2026-2620
Preprint. Discussion started: 20 May 2026

vary depending on background climate conditions and existing water stress. In some humid regions, increased evapotranspiration is offset by sufficient precipitation, maintaining stable water availability. In contrast, reforestation in already water limited areas, such as parts of Central Africa and Central America, can exacerbate dry season soil moisture deficits and reduce runoff, raising potential concerns for downstream water users. These spatial nuances highlight that the benefits and impact of reforestation extend beyond carbon uptake, underscoring the importance of integrating hydrological and socio-environmental considerations into land based climate mitigation strategies.

Code and data availability

All data generated for this study are available in the FRDR-DFDR repository (doi:10.20383/103.01657). The codes used to perform the calculations and produce the figures are available at: https://gitlab.com/Mortezapour/hydroclim_luc2.

Author contributions

KZ and MM conceptualized the research idea and designed the study. VKA contributed to the land model setup. MM developed and implemented the modelling and analytical methodology, performed data processing and calculations, visualized the results, and wrote the initial draft. CL contributed to data analysis. All authors discussed the results and edited the manuscript.

Competing interests

KZ and VKA are members of the editorial board of Earth System Dynamics.

Acknowledgements

This work made use of resources provided by the Collaborative Platform for CanESM (CP4C). CP4C is supported by funding from Environment and Climate Change Canada (ECCC, Project Number GCXE25S055) and uses computational resources provided by SciNet and the Digital Research Alliance of Canada (RPP #1234 [RPP2025]). CanESM is a project of ECCC. Computations were performed on the Niagara supercomputer at the SciNet HPC Consortium. SciNet is funded by Innovation, Science and Economic Development Canada; the Digital Research Alliance of Canada; the Ontario Research Fund – Research Excellence; and the University of Toronto (Ponce et al., 2019; Loken et al., 2010). We acknowledge the support of the NBSClimate project team and the Climate Research Lab at Simon Fraser University for helpful comments and discussions. ChatGPT (OpenAI) was used to support language refinement in limited sections of the manuscript. The authors take full responsibility for all scientific content and interpretations.

https://doi.org/10.5194/egusphere-2026-2620
Preprint. Discussion started: 20 May 2026

Financial Support

This project was undertaken with the financial support of the Government of Canada.

Ce projet a été réalisé avec l'appui financier du gouvernement du Canada.

References

Abe, M., Nozawa, T., Ogura, T., and Takata, K.: Effect of vegetation masking on future snow albedo reduction and its impact on surface warming in high latitude regions, Journal of Geophysical Research: Atmospheres, 122, 9353–9370, https://doi.org/10.1002/2017JD026957, 2017.

Amali, A. A., Schwingshackl, C., Ito, A., Barbu, A., Delire, C., Peano, D., Lawrence, D. M., Wårlind, D., Robertson, E., Davin, E. L., Shevliakova, E., Harman, I. N., Vuichard, N., Miller, P. A., Lawrence, P. J., Ziehn, T., Hajima, T., Brovkin, V., Zhang, Y., Arora, V. K., and Pongratz, J.: Biogeochemical versus biogeophysical temperature effects of historical land-use change in CMIP6, Earth System Dynamics, 16, 803–840, https://doi.org/10.5194/esd-16-803-2025, 2025.

Argaman, E., Karnieli, A., Zaady, E., Perevolotsky, A., Shachak, M., and Osem, Y.: Eco-hydrological functioning of multi-aged dryland afforestation systems, Journal of Soil and Water Conservation, 79, https://doi.org/10.2489/jswc.2024.00053, 2024.

Arora, V. K.: Simulating energy and carbon fluxes over winter wheat using coupled land surface and ecosystem models, Agricultural and Forest Meteorology, 118, 21–47, https://doi.org/10.1016/S0168-1923(03)00073-X, 2003.

Arora, V. K. and Boer, G. J.: A representation of variable root distribution in dynamic vegetation models, Earth Interactions, 7, 1–19, https://doi.org/10.1175/1087-3562(2003)007<0001:AROVRD>2.0.CO;2, 2003.

Arora, V. K. and Boer, G. J.: A parameterization of leaf phenology for the terrestrial ecosystem component of climate models, Global Change Biology, 11, 39–59, https://doi.org/10.1111/j.1365-2486.2004.00890.x, 2005.

Asselin, O., et al.: Blue in green: forestation turns blue water green, mitigating heat at the expense of water availability, Environmental Research Letters, 19, 114003, https://doi.org/10.1088/1748-9326/ad796c, 2024.

Bonan, G. B.: Forests and climate change: forcings, feedbacks, and the climate benefits of forests, Science, 320, 1444–1449, https://doi.org/10.1126/science.1155121, 2008.

Breil, M., Rechid, D., Davin, E. L., de Noblet-Ducoudré, N., Katragkou, E., Cardoso, R. M., Hoffmann, P., Jach, L. L., Soares, P. M. M., Sofiadis, G., Strada, S., Strandberg, G., Tölle, M. H., and Warrach-Sagi, K.: The opposing effects of

https://doi.org/10.5194/egusphere-2026-2620
Preprint. Discussion started: 20 May 2026

reforestation and afforestation on the diurnal temperature cycle, Journal of Climate, 33, 9159–9179, https://doi.org/10.1175/JCLI-D-19-0624.1, 2020.

Bright, R. M., Davin, E. L., O'Halloran, T. L., Pongratz, J., Zhao, K., and Cescatti, A..: Local temperature response to land cover and management change driven by non-radiative processes, Nature Climate Change, 13, 1052–1060, https://doi.org/10.1038/nclimate3250, 2017.

Brovkin, V., Claussen, M., Driesschaert, E., Fichefet, T., Kicklighter, D., Loutre, M. F., Matthews, H. D., Ramankutty, N., Schaeffer, M., and Sokolov, A.: Biogeophysical effects of historical land cover changes simulated by Earth system models, Climate Dynamics, 26, 587–600, https://doi.org/10.1007/s00382-005-0092-6, 2006.

Bruijnzeel, L. A.: Potential for improved groundwater recharge and dry-season flows under forest restoration, Hydrology and Earth System Sciences, 29, 1023–1045, https://doi.org/10.5194/hess-29-1023-2025, 2025.

Buechel, M., Osborne, T., Wilby, R. L., Dadson, S., Prudhomme, C., and Kay, A.: Broadleaf afforestation impacts on terrestrial hydrology insignificant compared to climate change, Hydrology and Earth System Sciences, 28, 2081–2103, https://doi.org/10.5194/hess-28-2081-2024, 2024.

Busch, J., Bukoski, J. J., Cook-Patton, S. C., Griscom, B., Kaczan, D., Potts, M. D., Yi, Y., Vincent, J. R., et al.: Cost-effectiveness of natural forest regeneration and plantations for climate mitigation, Nature Climate Change, 14, 1000–1010, https://doi.org/10.1038/s41558-024-02068-1, 2024.

Caporaso, L., Duveiller, G., Giuliani, G., Giorgi, F., Stengel, M., Massaro, E., Piccardo, M., and Cescatti, A.: Converging findings of climate models and satellite observations on European forests and cloud cover, Journal of Geophysical Research: Atmospheres, 129, e2023JD039235, https://doi.org/10.1029/2023JD039235, 2024.

Cerasoli, S., Vicente-Serrano, S. M., Sanchez-Lorenzo, A., Martin-Vide, J., Camarero, J. J., Beguería, S., and López-Moreno, J. I.: Cloud cooling effects of afforestation and reforestation at midlatitudes, Proceedings of the National Academy of Sciences, 118, e2026241118, https://doi.org/10.1073/pnas.2026241118, 2021.

Cho, K. H., Kim, Y., Byun, Y. H., Lee, M. I., and Kim, B. M.: Vegetation-cloud feedbacks to future vegetation changes in the Arctic regions, Atmospheric Chemistry and Physics, 18, 15081–15096, https://doi.org/10.5194/acp-18-15081-2018, 2018.

Cook-Patton, S. C., et al.: Mapping carbon potential from global natural forest regrowth, Nature, 585, 545–550, 2021.

https://doi.org/10.5194/egusphere-2026-2620
Preprint. Discussion started: 20 May 2026

Daley, J.: Reforestation done right is a multi-tasking climate solution, Frontiers in Forests and Global Change, 7, 1381078, https://doi.org/10.3389/ffgc.2024.1381078, 2024.

Davin, E. L. and de Noblet-Ducoudré, N.: Climatic impact of global-scale deforestation: radiative versus nonradiative processes, Journal of Climate, 23, 97–112, https://doi.org/10.1175/2009JCLI3102.1, 2010.

De Hertog, S. J., Davin, E. L., Boysen, L. R., Pongratz, J., and Lawrence, D. M.: Biogeophysical effects of idealized land cover and land management changes in Earth system models, Earth System Dynamics, 13, 1305–1324, https://doi.org/10.5194/esd-13-1305-2022, 2022.

De Hertog, S. J., Davin, E. L., Boysen, L. R., Pongratz, J., and Lawrence, D. M.: Effects of idealised land cover and land management changes on the atmospheric water cycle, EGUsphere [preprint], https://doi.org/10.5194/egusphere-2023-953, 2023.

Dubois, E., Minville, M., Trottier, G., and Leconte, R.: Impact of land cover changes on long-term regional-scale groundwater recharge simulation in cold and humid climates, Hydrological Processes, 37, e14711, https://doi.org/10.1002/hyp.14711, 2023.

Ellison, D., Futter, M. N., and Bishop, K.: On the forest cover-water yield debate: from demand- to supply-side thinking, Global Change Biology, 18, 806–820, https://doi.org/10.1111/j.1365-2486.2011.02589.x, 2012.

Engel, S., van der Ent, R. J., Keys, P. W., and van Noordwijk, M.: Can large-scale tree cover change negate climate change impacts on future water availability?, Hydrology and Earth System Sciences, 29, 1895–1918, https://doi.org/10.5194/hess-29-1895-2025, 2025.

Fahrenbach, N. L. S., Lawrence, D. M., Berg, A., Brovkin, V., Davin, E. L., and Boysen, L. R.: Mechanistic insights into tropical circulation and hydroclimate responses to future forest cover change, EGUsphere [preprint], https://doi.org/10.5194/egusphere-2025-1262, 2025.

FAO: Global Forest Resources Assessment 2020: Main report, Food and Agriculture Organization of the United Nations, 2020.

Frierson, D. M. W., Hwang, Y. T., and Kang, S. M.: Effects of Arctic sea ice loss on the atmospheric circulation: an energy balance perspective, Journal of Climate, 26, 2067–2080, https://doi.org/10.1175/JCLI-D-12-00033.1, 2013.

Green, B. and Marshall, J.: Coupling of trade winds with ocean circulation damps ITCZ shifts, Journal of Climate, 30, 4397–4411, https://doi.org/10.1175/JCLI-D-16-0812.1, 2017.

https://doi.org/10.5194/egusphere-2026-2620
Preprint. Discussion started: 20 May 2026

Griscom, B. W., et al.: Natural climate solutions, Proceedings of the National Academy of Sciences, 114, 11645–11650, https://doi.org/10.1073/pnas.1710465114, 2017.

Hoek van Dijke, A. J., Staal, A., Tuinenburg, O. A., and Dekker, S. C.: Shifts in regional water availability due to global tree restoration, Nature Geoscience, 15, 656–662, https://doi.org/10.1038/s41561-022-00935-0, 2022.

Hou, Y., Lei, H., Yang, D., and Piao, S.: A global synthesis of hydrological sensitivities to deforestation and forestation, Forest Ecology and Management, 532, 120718, https://doi.org/10.1016/j.foreco.2022.120718, 2023.

Hurtt, G. C., et al.: Harmonization of global land use change and management for the period 850–2100 (LUH2) for CMIP6, Geoscientific Model Development, 13, 5425–5464, https://doi.org/10.5194/gmd-13-5425-2020, 2020.

IPBES: Global assessment report on biodiversity and ecosystem services, Intergovernmental Science-Policy Platform on Biodiversity and Ecosystem Services, 2019.

King, J. A., Swart, N. C., Brovkin, V., Arora, V. K., Pongratz, J., Seneviratne, S. I., and Zickfeld, K.: Global and regional hydrological impacts of global forest expansion, Biogeosciences, 21, 3883–3902, https://doi.org/10.5194/bg-21-3883-2024, 2024.

Lal, R.: Soil carbon sequestration impacts on global climate change and food security, Science, 304, 1623–1627, 2018.

Li, Y., Zhao, M., Motesharrei, S., Mu, Q., Kalnay, E., and Li, S.: Biophysical effects of deforestation on climate via changes in clouds and radiation, Nature Communications, 15, 51783, https://doi.org/10.1038/s41467-024-51783-y, 2024.

Li, Y., Piao, S., Chen, A., Wang, X., Ciais, P., and Friedlingstein, P.: A global synthesis of hydrological sensitivities to deforestation and forestation, Forest Ecology and Management, 532, 120718, https://doi.org/10.1016/j.foreco.2022.120718, 2022.

Li, Y., Liu, Y., Xu, L., Chen, J., Wang, X., and Piao, S.: Using statistical models to depict drought response to forest cover change, Hydrology and Earth System Sciences, 28, 321–336, https://doi.org/10.5194/hess-28-321-2024, 2024.

Loken, C., et al.: SciNet: Lessons learned from building a power-efficient Top-20 system, Journal of Physics: Conference Series, 256, 012026, https://doi.org/10.1088/1742-6596/256/1/012026, 2010.

https://doi.org/10.5194/egusphere-2026-2620
Preprint. Discussion started: 20 May 2026

Meier, R., Davin, E. L., Lejeune, Q., Hauser, M., Martius, O., and Seneviratne, S. I.: Empirical estimate of forestation-induced precipitation changes in Europe, Nature Geoscience, 14, 473–478, https://doi.org/10.1038/s41561-021-00773-6, 2021.

Meinshausen, M., et al.: The shared socio-economic pathway (SSP) greenhouse gas concentrations, Geoscientific Model Development, 13, 3571–3605, https://doi.org/10.5194/gmd-13-3571-2020, 2020.

Ponce, M., et al.: Deploying a Top-100 supercomputer for large parallel workloads, PEARC'19 Proceedings, https://doi.org/10.1145/3332186.3332195, 2019.

Poorter, L., et al.: Biomass resilience of Neotropical secondary forests, Nature, 530, 211–214, 2016.

Portmann, R., Stuecker, M. F., McDermid, S. P., Good, P., and Booth, B. B. B.: Global forestation and deforestation affect remote climate, Nature Communications, 13, 5822, https://doi.org/10.1038/s41467-022-33279-9, 2022.

Robinson, N., et al.: Protect young secondary forests for optimum carbon removal, Nature Climate Change, 15, 793–800, 2025.

Schwärzel, K., et al.: How afforestation affects the water cycle in drylands, Global Change Biology, 26, 944–959, https://doi.org/10.1111/gcb.14875, 2020.

Swann, A. L. S., Fung, I. Y., and Chiang, J. C. H.: Mid-latitude afforestation shifts circulation and precipitation, Proceedings of the National Academy of Sciences, 107, 4911–4915, https://doi.org/10.1073/pnas.0911706107, 2010.

Swart, N. C., et al.: The Canadian Earth System Model version 5 (CanESM5.0.3), Geoscientific Model Development, 12, 4823–4873, https://doi.org/10.5194/gmd-12-4823-2019, 2019.

Winckler, J., Reick, C. H., and Pongratz, J.: Robust identification of local biogeophysical effects, Journal of Climate, 32, 5477–5495, https://doi.org/10.1175/JCLI-D-18-0819.1, 2019.

van Meerveld, H. J. I.: Reforestation effects on low flows, WIREs Water, 12, e1760, https://doi.org/10.1002/wat2.1760, 2025.

Verseghy, D. L.: A Canadian land surface scheme for GCMs. I. Soil model, International Journal of Climatology, 11, 111–133, https://doi.org/10.1002/joc.3370110202, 1991.

https://doi.org/10.5194/egusphere-2026-2620
Preprint. Discussion started: 20 May 2026

Verseghy, D. L., McFarlane, N. A., and Lazare, M.: CLASS—A Canadian land surface scheme for GCMs, II, International Journal of Climatology, 13, 347–370, https://doi.org/10.1002/joc.3370130402, 1993.

Verseghy, D. L.: The Canadian Land Surface Scheme (CLASS): Its history and future, Atmosphere-Ocean, 38, 1–13, https://doi.org/10.1080/07055900.2000.9649637, 2000.

Xu, R., Zhang, Y., Wang, X., Yang, Y., Chen, J., and Piao, S.: Contrasting impacts of forests on cloud cover, Nature Communications, 13, 444, https://doi.org/10.1038/s41467-022-28161-7, 2022.

Zan, B., Staal, A., Tuinenburg, O. A., Keys, P. W., and Dekker, S. C.: Spatiotemporal inequality in land water availability, Nature Water, 2, 345–355, https://doi.org/10.1038/s44221-024-00296-5, 2024.

Zhang, Y., Peña-Arancibia, J. L., McVicar, T. R., Chiew, F. H. S., Vaze, J., Liu, C., et al.: Multi-decadal trends in global terrestrial evapotranspiration, Scientific Reports, 6, 19124, https://doi.org/10.1038/srep19124, 2017.